Level Set Methods for Curvature Flow, Image Enchancement, and Shape Recovery in Medical Images *

R. Malladi and J.A. Sethian †

Department of Mathematics
and
Lawrence Berkeley Laboratory
University of California, Berkeley, California 94720

To appear, Proceedings of Conference on Visualization and Mathematics:
June, 1995, Berlin, Germany

Abstract

Level set methods are powerful numerical techniques for tracking the evolution of interfaces moving under a variety of complex motions. They are based on computing viscosity solutions to the appropriate equations of motion, using techniques borrowed from hyperbolic conservation laws. In this paper, we review some of the applications of this work to curvature motion, the construction of minimal surfaces, image enhancement, and shape recovery. We introduce new schemes for denoising three-dimensional shapes and images, as well as a fast shape recovery techniques for three-dimensional images.

1 Introduction

In a variety of problems, the goal is to track a propagating front which can form sharp corners and cusps, change topology, break and merge as it evolves. Such phenomena can occur in fluid mechanics, material science, the microfabrication of electronic components, combustion, meteorology, control theory, and image processing, as well as more mathematical problems in minimal surfaces and construction of geodesics. Level set methods, introduced in [22], have been applied a wide range of such problems, providing powerful tools for tracking some of the most complex phenomena. For a review of level set methods in many contexts, see [32]; for an introductory text, see the recent book by Sethian [33]. In this paper, we briefly introduce level set methods, and discuss their application to some

*Correct citation: Malladi, R., and Sethian, J.A., Proc. of Conf. on Visualization and Mathematics, June, 1995, Berlin, Germany, Springer-Verlag, Heidelberg, Germany, pp. 329–345, 1997.

†Supported in part by the Applied Mathematics Subprogram of the Office of Energy Research under contract DE-AC03-76SF00098, and the National Science Foundation and DARPA under grant DMS-8919074.

particular problems on the boundary of visualization and mathematics. We discuss problems in curvature flow, minimal surfaces, and self-similar surfaces, applications to image enhancement, and shape recovery in medical images.

2 Level Set Methods

2.1 Background

A variety of standard numerical algorithms are available to advance interfaces. These methods are not unique to a particular field, and are in use in such areas as dendritic growth and solidification, flame/combustion models, and fluid interfaces. Roughly speaking, they fall into the three general categories of marker/strings methods, volume-of-fluid methods, and characteristic methods. All three are plagued by stability problems, difficulty in accurately determining curvatures and normals, and complexities in three dimensions.

Level set methods, introduced by Osher and Sethian in [22], offer a highly robust and accurate method for tracking interfaces moving under complex motions. Their major virtue is that they naturally construct the fundamental weak solution to surface propagation posed by Sethian [24, 25]. They work in any number of space dimensions, handle topological merging and breaking naturally, and are easy to program. They approximate the equations of motion for the underlying propagating surface, which resemble Hamilton-Jacobi equations with parabolic right-hand sides. The central mathematical idea is to view the moving front as a particular level set of a higher dimensional function. In this setting, sharp gradients and cusps can form easily, and the effects of curvature may be easily incorporated. The key numerical idea is to borrow the technology from the numerical solution of hyperbolic conservation laws and transfer these ideas to the Hamilton-Jacobi setting, which then guarantees that the correct entropy-satisfying solution will be obtained.

2.2 Formulation

Consider a boundary, either a curve in two dimensions or a surface in three dimensions, separating one region from another, and imagine that this curve/surface moves in its normal direction with a known speed function F. The goal is to track the motion of this interface as it evolves. We are only concerned with the motion of the interface in its normal direction, and shall ignore tangential motion.

Given an initial position for an interface Γ, where Γ is a closed curve in R^2, and a speed function F which gives the speed of Γ in its normal direction, the level set method takes the perspective of viewing Γ as the zero level set of a function $\phi(x, t = 0)$ from R^2 to R. That is, let $\phi(x, t = 0) = \pm d$, where d is the distance from x to Γ, and the plus (minus) sign is chosen if the point x is outside (inside) the initial hypersurface Γ. Then, by the chain rule, an evolution equation for the interface may be produced [22, 27], namely

$$\phi_t + F|\nabla\phi| = 0, \tag{1}$$

$$\phi(x, t = 0) = given. \tag{2}$$

This is an initial value partial differential equation in one higher dimension than the original problem.[1] In Figure 1 (taken from [28]), we show the outward propagation of an initial curve and the accompanying motion of the level set function ϕ. There are several

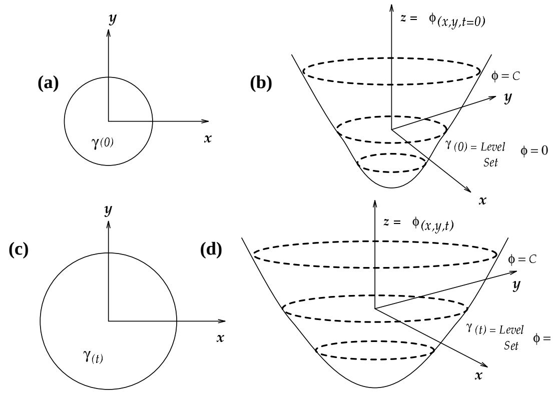

Figure 1: Propagating Circle

advantages to this level set perspective:

1. Although $\phi(x,t)$ remains a function, the level surface $\phi = 0$ corresponding to the propagating hypersurface may change topology, as well as form sharp corners as ϕ evolves (see [22]).

2. Second, a discrete grid can be used together with finite differences to devise a numerical scheme to approximate the solution. Care must taken to adequately account for the spatial derivatives in the gradient.

3. Third, intrinsic geometric properties of the front are easily determined from the level set function ϕ. The normal vector is given by $\vec{n} = \frac{\nabla\phi}{|\nabla\phi|}$ and the curvature of each level set is $\kappa = \nabla \cdot \frac{\nabla\phi}{|\nabla\phi|}$.

4. Finally, the formulation is unchanged for propagating interfaces in three dimensions.

Since their introduction in [22], level set techniques have been used in a wide collection of problems involving moving interfaces. Some of these applications include the generation of minimal surfaces [7], singularities and geodesics in moving curves and surfaces in [9], flame propagation [23, 36], as well as etching, deposition and lithography calculations in [2, 3]. Extensions of the basic technique include fast methods in [1], level set techniques for multiple fluid interfaces and triple point junctions in [30], crystal growth [35], and grid generation in [28]. The fundamental Eulerian perspective presented by this approach has since been adopted in many theoretical analyses of mean curvature flow, in particular, see [10, 6]. A particularly fast version which applies to the special case of a monotonically advancing front may be found in [32, 31].

[1] this is a particular form of the more general *Hamilton-Jacobi* equation which can be abstractly written as $\phi_t + H(\phi_x, \phi_y)$.

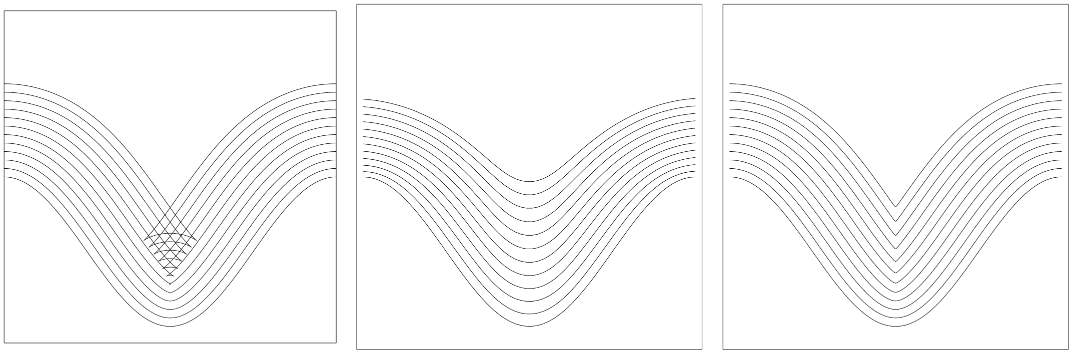

$Swallowtail(F = 1.0)$ $F = 1. - 0.25\kappa$ $Entropy\,Solution(F = 1.0)$

Figure 2: Cosine Curve Propagating with Unit Speed

2.3 Numerical Approximation

2.3.1 Shocks, Entropy Conditions, Curvature and Viscosity

The crucial issue in the numerical approximation of the level set equation is the realization that the evolving curve/surface can develop corners where the evolving interfaces focuses, rarefaction fans where it expands, and regions where it changes topology. The key to constructing numerical techniques which correctly handle these mechanisms is to construct what are known as "entropy-satisfying" approximations to the gradient term in Eqn. 1.

As shown in [24, 25, 27], a propagating interface can develop corners and discontinuities as it evolves, which require the introduction of a weak solution in order to proceed. The correct weak solution comes from enforcing an entropy condition posed by Sethian [25] for the propagating interface, similar to the one in gas dynamics. Furthermore, this entropy-satisfying weak solution is the one obtained by considering the limit of smooth solutions for the problem in which curvature plays a regularizing role.

As an example, consider the initial cosine curve propagating with speed $F = 1$ shown in Figure 2. As the front moves, a corner forms in the propagating front which corresponds to a shock in the slope, and a weak solution must be developed beyond this point. If the motion of each individual point is continued, the result is the swallowtail solution shown in Fig. 2a, which is multiple-valued and does not correspond to a clear interface separating two regions. Instead, an appropriate weak solution is obtained by considering the associated smooth flow obtained by adding curvature κ to the speed law, that is, letting $F = 1 - \epsilon\kappa$, see Fig. 2b. The limit of these smooth solutions as ϵ goes to zero produces the weak solution shown in Fig. 2c.

Another way to obtain this same solution is through enforcing an entropy condition posed by Sethian [24], similar to the one for a scalar hyperbolic conservation law. Imagine that the front is the boundary of a propagating flame, separating a burning region below from an unburnt region above. The front at any time t is the just the set of all points located a distance t from the initial front. Thus, the entropy condition may be stated briefly as "once a point burns, it stays burnt", see [24]. This weak solution corresponds to a decrease in total variation of the propagating front and is irreversible [25]. For details, see [25].

Since the entropy condition is similar to the one for hyperbolic conservation laws, as a numerical technique it suggests using that technology to solve the equations of motion, as described in [26].

2.3.2 Entropy-satisfying upwind differences schemes

As a simple case, let $F(\kappa) = 1$ and consider the initial value problem

$$\psi_t = (1 + \psi_x^2)^{1/2}, \tag{3}$$

$$\psi(x, 0) = f(x) = \left\{ \begin{array}{ll} 1/2 - x & x \leq 1/2 \\ x - 1/2 & x > 1/2 \end{array} \right\}. \tag{4}$$

This is the equation of motion of the height ψ of a function which always remains a graph as it moves in its normal direction with speed F.

We focus on the gradient term $(1 + {\psi_x}^2)$ (we call this a gradient term because ψ_x is the one-dimensional gradient. One approach is to use a central difference approximation to the gradient term, namely

$$\psi_t \approx \frac{\psi_i^{n+1} - \psi_i^n}{\Delta t} = [1 + [\frac{\psi_{i+1}^n - \psi_{i-1}^n}{2\Delta x}]^2]^{1/2} = [1 + [D_i^{0x}\psi]^2]^{1/2} \tag{5}$$

where in the last expression we have used standard notation for the central difference. Since $x_M = 1/2$, by symmetry, $\psi_{M+1} = \psi_{M-1}$, thus the right-hand-side is 1. However, for all $x \neq 1/2$, ψ_t is correctly calculated to be $\sqrt{2}$, since the graph is linear on either side of the corner and thus the central difference approximation is exact. Note that this has nothing to do with the size of the space step Δx or the time step Δt. *No matter how small we take the numerical parameters, as long as we use an odd number of points, the approximation to ψ_t at $x = 1/2$ gets no better.* It is simply due to the way in which the derivative ψ_x is approximated.

Consider now the following finite difference approximation introduced by Osher and Sethian [22]

$${\psi_x}^2 \approx (\max(D_i^{+x}\psi, 0)^2 + \min(D_i^{-x}\psi, 0)^2) \tag{6}$$

where we have used standard finite difference notation that

$$D_i^{-x}\psi = \frac{\psi_i - \psi_{i-1}}{h} \qquad D_i^{+x}\psi = \frac{\psi_{i+1} - \psi_i}{h} \tag{7}$$

where ψ_i is the value of ψ on a grid at the point ih with grid spacing h.

Eqn. 6 is an "upwind" scheme (see [33]); it chooses grid points in the approximation in terms of the direction of the flow of information. Intuitively, upwind means that if a wave progresses from left to right, then one should use a difference scheme which reaches *upwind* to the left in order to get information to construct the solution *downwind* to the right (see [33]). If we imagine a "V" curve propagating with speed $F = 1$ in its normal direction, we see that at the symmetric point, the symmetry of the scheme is changed, and a non-zero value is chosen, and the entropy condition is satisfied.

While a vast array of other upwind, entropy-satisfying schemes are available to approximate the gradient, for our purposes, the above approximation (and one small variation) will be sufficient. More details on upwind schemes, hyperbolic conservation laws, and their role in level set equations may be found in [25, 32, 33].

2.3.3 The General Level Set Scheme

Based on the above approximation to the gradient, we can now write down difference schemes for the level set equation. If one initializes the level set function with the signed distance function and ϕ negative on the inside, the direction of upwinding changes signs in the above approximation to the gradient, and we have (in three dimensions)

$$\phi_{ijk}^{n+1} = \phi_{ijk}^{n} - \Delta t[\max(F_{ijk}, 0)\nabla^{+} + \min(F_{ijk}, 0)\nabla^{-}] \tag{8}$$

where

$$\begin{aligned}\nabla^{+} = [\,&\max(D_{ijk}^{-x}, 0)^2 + \min(D_{ijk}^{+x}, 0)^2 + \\ &\max(D_{ijk}^{-y}\phi, 0)^2 + \min(D_{ijk}^{+y}\phi, 0)^2 + \\ &\max(D_{ijk}^{-z}\phi, 0)^2 + \min(D_{ijk}^{+z}\phi, 0)^2]^{1/2}\end{aligned} \tag{9}$$

$$\begin{aligned}\nabla^{-} = [\,&\max(D_{ijk}^{+x}\phi, 0)^2 + \min(D_{ijk}^{-x}\phi, 0)^2 + \\ &\max(D_{ijk}^{+y}\phi, 0)^2 + \min(D_{ijk}^{-y}\phi, 0)^2 + \\ &\max(D_{ijk}^{+z}\phi, 0)^2 + \min(D_{ijk}^{-z}\phi, 0)^2]^{1/2}.\end{aligned} \tag{10}$$

where $\phi(x, y, z, 0) = \pm d$.

This method updates the level set function ϕ by advancing the solution one time step using a first order forward Euler scheme. This method can be made much faster through the use of so-called "narrow-band methods", see [7, 21, 1].

3 Motion under Curvature, Self-Similar Flows, and Minimal Surfaces

In this section, we discuss a few applications of level set methods to pure geometry problems. We begin by focussing on a special speed function, namely $F = -\kappa$, where κ is the curvature. This corresponds to a geometric version of the heat equation; large oscillations are immediately smoothed out, and long-term solutions correspond to dissipation of all information about the initial state.

The remarkable work of Gage and Grayson investigated the motion of a simple closed curve collapsing under its curvature. First, Gage [11, 12] showed that any convex curve moving under such a motion remains convex and must shrink to a point. Grayson [13] followed this work with a stunning proof that *all* curves must shrink to a round point, regardless of their initial shape.

In Figure 3, we take an odd-shaped initial curve and view this as the zero level set of a function defined in all of R^2. Here, for illustration, we have ϕ such that $\phi < 0$ as black and $\phi > 0$ as white, thus the zero level set is the boundary between the two. As the level curves flow under curvature, the ensuing motion carries each to a point which then disappears. In the evolution of the front, one clearly sees that the large oscillations disappear quickly, and then as the front becomes circular, motion slows, and the front eventually disappears.

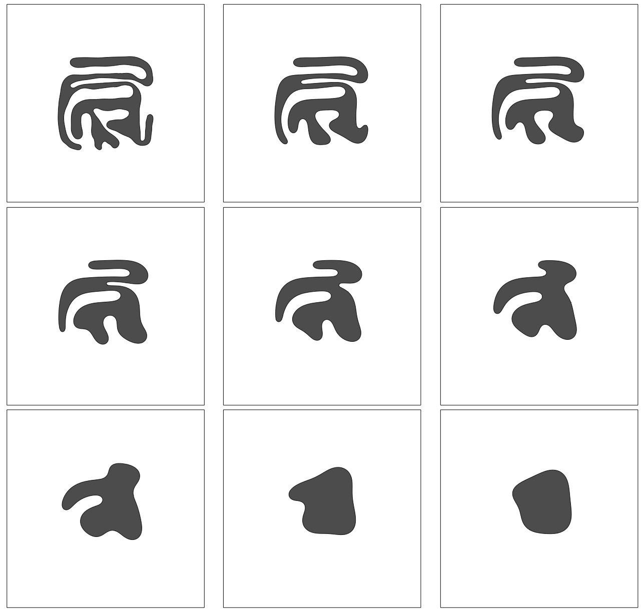

Figure 3: $F(\kappa) = -\kappa$:

In three dimensions, flow under mean curvature does not necessarily result in a collapse to a sphere. Huisken [15] showed that convex shapes shrink to spheres as they collapse, analogous to the result of Gage. However, Grayson showed that non-convex shapes may in fact *not* shrink to a sphere [14], and provided the counterexample of the dumbbell. A narrow handle of a dumbbell may have such a high inner radius that the mean curvature of the saddle point at the neck may still be positive, and hence the neck will pinch off.

As illustration, in Figure 4, taken from [9], we show two connected dumbbells collapsing under mean curvature. As the intersection point collapses, the necks break off and leave a remaining "pillow"-like region behind. This pillow region collapses as well, and eventually all five regions disappear.

What about self-similar shapes? In two dimensions, it is clear that a circle collapsing under its own curvature remains a circle, this can be seen by integrating the ordinary differential equation for the changing radius. In three dimensions, a sphere is self-similar under mean curvature flow, since its curvature is always constant. Angenent [5] proved the existence a self-similar torus which preserves the balance between the competing pulls towards a ring and a sphere.

In order to devise an algorithm to produce self-similar shapes, two things are required. First, since hypersurfaces get smaller as they move under their curvature, a mechanism is needed to "rescale" their motion so that the evolution can be continued towards a possible self-similar shape. And second, a way of pushing the evolving fronts back towards self-similarity is required. Chopp has accomplished both in a clever numerical algorithm that produces a family of self-similar surfaces, see [8]. His family comes from taking regular polyhedra (for example, a cube), and drilling holes in each face. The resulting figure then evolves according to auxiliary level set equation which contains the re-scaling as part of the equation of motion. One such self-similar surface is shown in Figure 5. For many more such

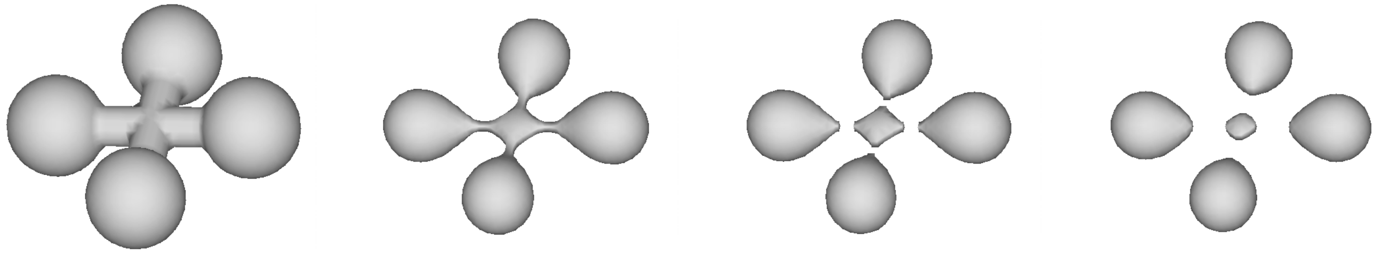

Figure 4: Collapse of Two-handled Dumbbell

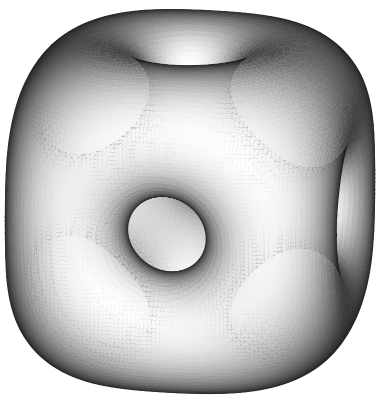

Self − Similar Cube with Holes
Fig. 5a

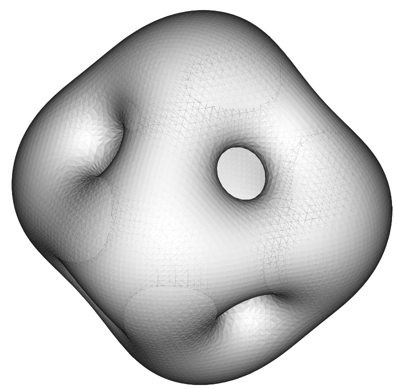

Self − Similar Octahedron with Holes
Fig. 5b

Figure 5: Self-Similar Shapes

shapes, see Chopp [8].

Finally, we turn to the construction of minimal surfaces. Consider a closed curve $\Gamma(s)$ in R^3. The goal is to construct a membrane with boundary Γ and mean curvature zero. In some cases, this can be achieved by as follows. Given the bounding wire frame Γ, consider some initial surface $S(t = 0)$ whose boundary is Γ. Let $S(t)$ be the family of surfaces parameterized by t obtained by allowing the initial surface $S(t = 0)$ to evolve under mean curvature, with boundary always given by Γ. Defining the surface S by $S = \lim_{t\to\infty} S(t)$, one expects that the surface S will be a minimal surface for the boundary Γ.

A level set approach to this problem rests on embedding the motion of the surface towards its minimal energy as the zero level set of a higher dimensional function. Thus, given an initial surface $S(0)$ passing through Γ, construct a family of neighboring surfaces by viewing $S(0)$ as the zero level set of some function ϕ over all of R^3. Using the level set equation (Eqn. 1), evolve ϕ according to the speed law $F(\kappa) = -\kappa$. Then a possible

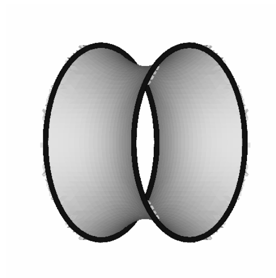

Figure 6: Minimal Surface: Catenoid

minimal surface S will be given by

$$S = \lim_{t \to \infty} \{x | \phi(x,t) = 0\} \tag{11}$$

The difficult challenge with the above approach is to ensure that the evolving zero level set always remains attached to the boundary Γ. This is accomplished by Chopp [7] by creating a set of boundary conditions on those grid points closest to the wire frame that link together the neighboring values of ϕ to force the level set $\phi = 0$ through Γ. Thus, the problem turns into one of constrained level set problem; we track mean curvature flow with the constraint the evolving zero level set remained attached to the front.

In Figure 6, taken from [7], the minimal surface spanning two rings each of radius 0.5 and at positions $x = \pm.277259$ is computed. A cylinder spanning the two rings is taken as the initial level set $\phi = 0$. A $27 \times 47 \times 47$ mesh with space step 0.025 is used. The final shape is shown in from several different angles in Figure 6.

Next, in Figure 7 (again taken from [7]), this same problem is computed, but the rings are placed far enough apart so that a catenoid solution cannot exist. Starting with a cylinder as the initial surface, the evolution of this surface is computed as it collapses under mean curvature while remaining attached to the two wire frames. As the surface evolves, the

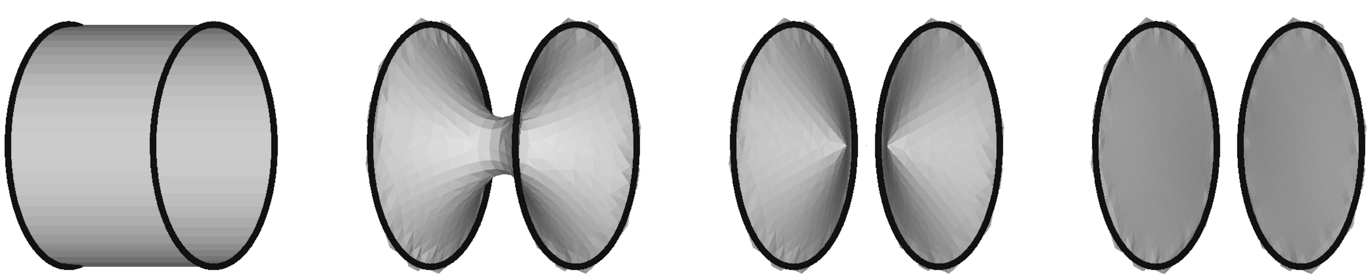

$Time = 0.0$ $\quad$ $Time = 0.41$ $\quad$ $Time = 0.42$ $\quad$ $Time = 0.50$

Figure 7: Splitting of Catenoid

middle pinches off and the surface splits into two surfaces, each of which quickly collapses into a disk. The final shape of a disk spanning each ring is indeed a minimal surface for this problem. This example illustrates one of the virtues of the level set approach. No special cutting or *ad hoc* decisions are employed to decide when to break the surface. Instead, viewing the zero level set as but one member of a family of flowing surfaces allows this smooth transition. Further results may be found in [7].

4 Image Enchancement and Noise Removal

A very different application of these techniques is in image enchancement and denoising. Define an *image* to be an intensity map $I(x, y)$ given at each point of a two-dimensional domain. The range of the function $I(x, y)$ depends on the type of image; for black and white image the range is either 0 or 255, for grey-scale images $I(x, y)$ is a function mapped between 0 and 255. Alvarez, Lions and Morel ([4]) introduced a noise removal scheme by employing, in part, some of the above ideas about curvature flow and level set equations. Their basic idea was to flow iso-intensity contours under curvature flow; An attractive quality of this motion is that sharp boundaries are preserved; smoothing takes place inside a region, but not across region boundaries. Of course, as shown by Grayson's theorem, eventually all information is removed as each contour shrinks to zero and disappears.

In Malladi and Sethian [17, 18], a curvature-based flow algorithm was developed which avoids these problems; the scheme results from returning to the original ideas of curvature flow, and exploiting a "min/max" function which correctly selects the optimal motion to remove noise. It has two highly desirable features:

1. There is an intrinsic, adjustable definition of scale within the algorithm, such that all noise below that level is removed, and all features above that level are preserved.

2. The algorithm stops automatically once the sub-scale noise is removed; continued application of the scheme produces no change.

. We now describe this algorithm in some detail.

4.1 Noise removal from two-dimensional images

To understand this scheme, consider the equation

$$\phi_t = \bar{F}|\nabla\phi|. \tag{12}$$

A curve collapsing under its curvature will correspond to speed $\bar{F} = \kappa$. Now, consider two variations on the basic curvature flow, namely

- $\bar{F}(\kappa) = \min(\kappa, 0.0)$
- $\bar{F}(\kappa) = \max(\kappa, 0.0)$

Here, we have chosen the negative of the signed distance in the interior, and the positive sign in the exterior region. The effect of flow under $\bar{F}(\kappa) = \min(\kappa, 0.0)$ is allow the inward concave fingers to grow outwards, while suppressing the motion of the outward convex regions. Thus, the motion halts as soon as the convex hull is obtained. Conversely, the

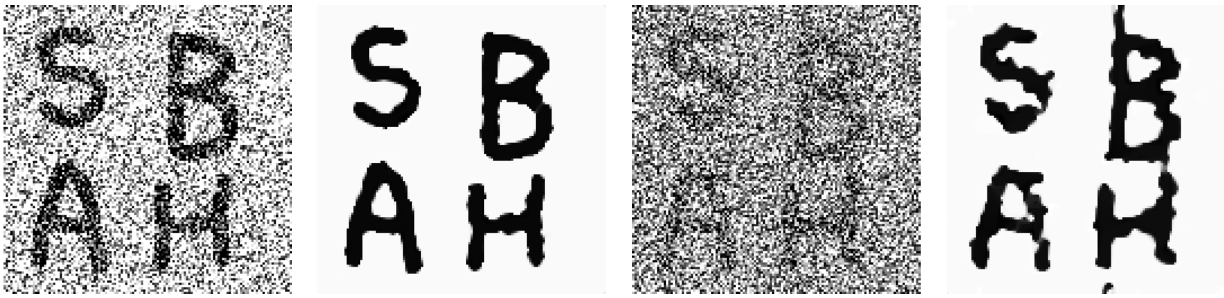

50.0% *Noise* | *Restored* | 80.0% *Noise* | *Restored*

Figure 8: Image restoration of Binary Images with Grey-Scale Salt-and-Pepper Noise Using Min/Max Flow: Restored shapes are final shape obtained ($T = \infty$).

effect of flow under $\bar{F}(\kappa) = \max(\kappa, 0.0)$ is to allow the outward regions to grow inwards while suppressing the motion of the inward concave regions. However, once the shape becomes fully convex, the curvature is always positive and the flow becomes the same as regular curvature flow.

Our goal is to select the correct choice of flow that smoothes out small oscillations, but maintains the essential properties of the shape. In order to do so, we discuss the idea of the min/max switch.

Consider the following speed function, introduced in [17] and refined considerably in [18]:

$$\bar{F}^{Stencil=k}_{\min/\max} = \begin{cases} \min(\kappa, 0) & \text{if } Ave^{R=kh}_{\phi(x,y)} < 0 \\ \max(\kappa, 0) & \text{if } Ave^{R=kh}_{\phi(x,y)} \geq 0 \end{cases} \tag{13}$$

where $Ave^{R=kh}_{\phi(x,y)}$ is defined as the average value of ϕ in a disk of radius $R = kh$ centered around the point (x, y). Here, h is the step size of the grid. Thus, given a "StencilRadius" k, the above yields a speed function which depends on the value of ϕ at the point (x, y), the average value of ϕ in neighborhood of a given size, and the value of the curvature of the level curve going through (x, y).

In Figure 8, 50% and 80% grey-scale noise is added to a black and white image of a hand-written character. The noise is added as follows: $X\%$ noise means that at $X\%$ of the pixels, the given value is replaced with a number chosen with uniform distribution between 0 and 255. Here, the min/max switch function is taken relative to the value 127.5 rather than zero. The restored figures are converged. Continued application of the scheme yields almost no change in the results. We refer the reader to Malladi and Sethian [18, 19] for further applications of this scheme in enhancement of grey-scale and color images, edge finding, and its link to accurate shape recovery.

4.2 Noise removal in 3D

There is an obvious extension of the above scheme to 3D in order to denoise surfaces and CT & MRI images of the form $I(x, y, z)$. Flowing level surfaces of a function under mean

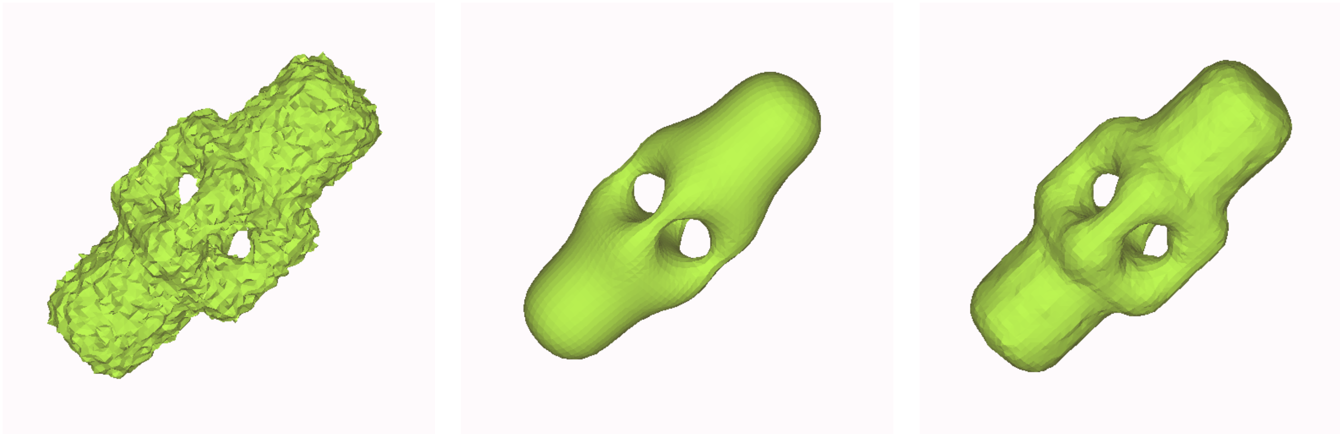

(a) Noisy Surface (b) $F = H$ (c) $F = \bar{F}_{Min/Max}$

Figure 9: Min/Max flow on surfaces

curvature will smooth the surfaces but will eventually cause them to shrink, sometimes split, and collapse. As an alternative, we take the following approach.

Let us represent an initial noisy surface as the zero level set of a function $\phi(x, y, z)$. Our goal is to smooth this surface without loosing the essential structure of the surface. We do this by moving the surface under a combination of two flows, $\min(H, 0)$ and $\max(H, 0)$ based on a local decision. Specifically, the speed $\bar{F}$ at every point is defined to be:

$$\bar{F} = \begin{cases} \max(H, 0) & \text{if } Ave^{R=kh}_{\phi(x,y,z)} < T \\ \min(H, 0) & \text{if } Ave^{R=kh}_{\phi(x,y,z)} \geq T \end{cases} \tag{14}$$

where T at every point is a "threshold" which gives a sense of the background region into which the boundary perturbation should be diffused. We compute T by averaging along a circle, centered at the current point and lying on the tangent plane. This construction ensures that the points used in the computation always lie on the same side of the surface. Again, by increasing the size of the averaging window, we define a family of flows that are capable of removing larger and larger structures from the surface.

As an example, consider the noisy surface shown in Figure 9a. This surface represented on a $64 \times 64 \times 64$ grid and moved under its mean curvature for 50 time steps is shown in Figure 9b. Clearly, the surface is completely diffused resulting in considerable loss in volume. On the other hand, the surface in Figure 9c is the result of running our min / max flow given in Eqn. 14. An identical calculation can be employed to denoise 3D medical images.

5 Shape Recovery

5.1 Background

Imagine that one is given an image. The goal in *shape detection/recovery* is to extract a particular shape from that image; here, "extract" means to produce a mathematical description of the shape which can be used in a variety of forms. The work on level set techniques applied to shape recovery described here was first presented in Malladi, Sethian, and Vemuri [20]; further work using the level set scheme in the context of shape recovery may be found in [21, 17]. We refer the interested reader to those papers for motivation, details, and a large number of examples.

Imagine that we are given an image, with the goal of isolating a shape within the image. Our approach (see [21]) is motivated by the active force contour/snake approach to shape recovery given in [16]. We start an initial front inside the desired region, and let it propagate outwards with a speed function that stops the motion when the boundary is reached.

More precisely, consider a speed function of the form $1 - \epsilon\kappa$ $(-1 - \epsilon\kappa)$, where ϵ is a constant. As discussed earlier, the constant acts as an advection term, and is independent of the moving front's geometry. The front uniformly expands (contracts) with speed 1 (-1) depending on the sign, and is analogous to an inflation force. The diffusive second term ϵK depends on the geometry of the front and smooths out the high curvature regions of the front. It has the same regularizing effect on the front as the internal deformation energy term in thin-plate-membrane splines [16].

Our goal now is to define a speed function from the image data that acts as a halting criterion for this speed function. Here, we extend the original work in [21] to three dimensions. The surface moves under a simple speed law $F = 1 - \epsilon H$, where H is the mean curvature given by the following expression:

$$H = \frac{\psi_{xx}(\psi_y^2 + \psi_z^2) + \psi_{yy}(\psi_x^2 + \psi_z^2) + \psi_{zz}(\psi_x^2 + \psi_y^2) - 2\psi_{xy}\psi_x\psi_y - 2\psi_{yz}\psi_y\psi_z - 2\psi_{zx}\psi_z\psi_x}{(\psi_x^2 + \psi_y^2 + \psi_z^2)^{3/2}}. \tag{15}$$

The objective is to mold the initial surface into desired anatomical shapes by solving an initial value partial differential equation on the function ψ. The driving force for this comes from applying artificial image-based speed terms on the surface. We use two such terms. The first one is a term that causes the surface to stop in the vicinity of desired shape boundaries and the second term attracts the surface towards the same boundaries; the latter has a stabilizing effect. Specifically, the equation of motion is

$$\psi_t + k_I(1 - \epsilon H)|\nabla\psi| - \beta\nabla P \cdot \nabla\psi = 0. \tag{16}$$

Here, the term

$$k_I = \frac{1}{1 + \mid \nabla G_\sigma * I(x,y,z) \mid} \tag{17}$$

causes the surface to have speeds very close to 0 near high image gradients, i.e., possible edges. False gradients due to noise can be avoided by applying a Gaussian smoothing filter or more sophisticated edge-preserving smoothing schemes (see [17, 18]). The second term $\nabla P \cdot \nabla\psi$ denotes the projection of an (attractive force) vector normal to the surface. This force which is realized as the gradient of a potential field

$$P(x,y,z) = -|\nabla G_\sigma * I(x,y,z)|, \tag{18}$$

attracts the surface to the edges in the image; coefficient β controls the strength of this attraction.

5.2 Results

First, we consider a CT image of human thighs. The objective is to reconstruct and visualize the shapes of both the thighs and the thigh bones. In Figure 10, we depict an evolutionary

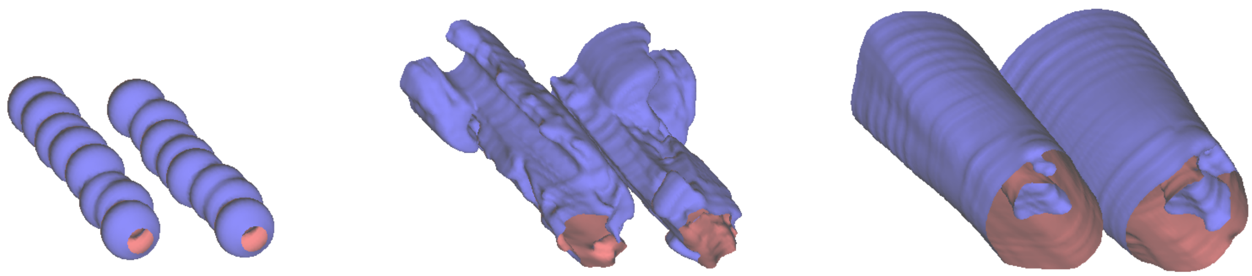

(a) Initial (b) Rapidly Evolving (c) Final

Figure 10: Evolutionary sequence depicting the reconstruction of human thigh starting from an initial shape shown in part (a).

sequence of the reconstruction of the femurs and surrounding soft tissue. Computation was performed at the same resolution as the initial data on a $128 \times 128 \times 61$ grid.

In the next example we recover the shapes of heart chambers from MRI data. The data is given as a time sequence of images of the form $I(x, y, z)$ and the objective is to depict the shapes of right and left ventricle. Such calculations are important both to visualize and to quantify the change in volume of the heart chambers. Figure 11 shows a sequence of nine cardiac configurations reconstructed from a time sequence of MRI images at the grid resolution of $256 \times 256 \times 10$.

Acknowledgements: The contributions of David Adalsteinsson and his fast narrow band version of the level set code are gratefully acknowledged.

References

[1] Adalsteinsson, D., and Sethian, J.A., *A Fast Level Set Method for Propagating Interfaces*, J. Comp. Phys., Vol. 118(2), pp. 269–277, May 1995.

[2] Adalsteinsson, D., and Sethian, J.A., *A Unified Level Set Approach to Etching, Deposition and Lithography I: Algorithms and Two-dimensional Simulations*, Vol. 120, No. 1, pp. 128-144, 1995.

[3] Adalsteinsson, D., and Sethian, J.A., *A Unified Level Set Approach to Etching, Deposition and lithography II: Three-dimensional Simulations*, J. Comp. Phys., 122, 2, pp. 348-366, 1995.

[4] Alvarez, L., Lions, P.L., and Morel, M., *Image Selective Smoothing and Edge detection by Nonlinear Diffusion. II,* SIAM Journal on Numerical Analysis, Vol. 29(3), pp. 845–866, 1992.

[5] Angenent, S.,*Shrinking Doughnuts*, in "Proceedings of Nonlinear Diffusion Equations and Their Equilibrium States", 3, (Edited by N.G. Lloyd et. al.), Birkhauser, Boston, 1992.

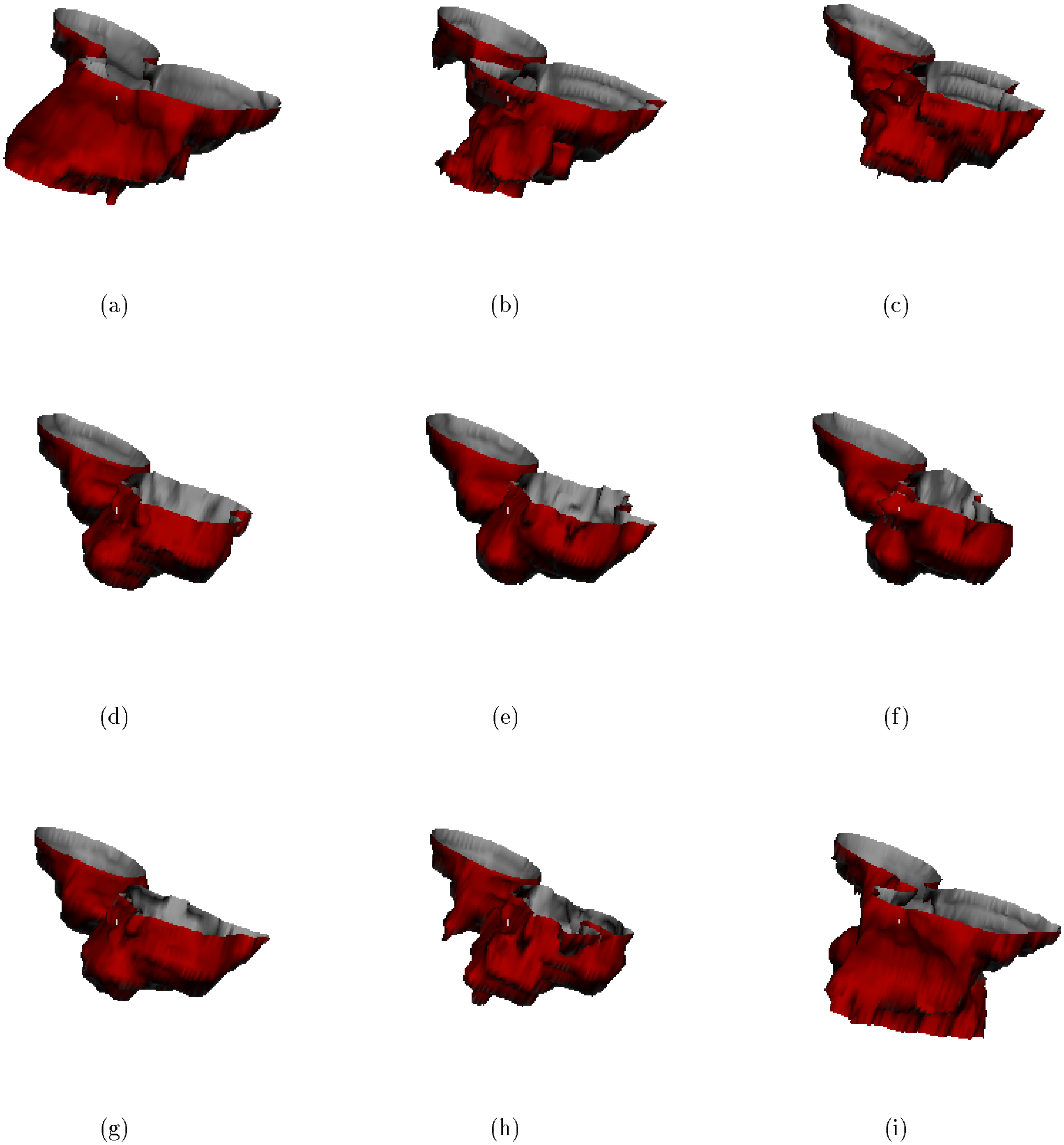

Figure 11: Heart chamber reconstruction from a time sequence of MRI images

[6] Chen, Y., Giga, Y., and Goto, S., *Uniqueness and Existence of Viscosity Solutions of Generalized Mean Curvature Flow Equations*, J. Diff. Geom, Vol. 33, 749, 1991.

[7] Chopp, D.L., *Computing Minimal Surfaces via Level Set Curvature Flow*, Jour. of Comp. Phys., Vol. 106, pp. 77–91, 1993.

[8] Chopp, D.L., *Numerical Computation of Self-Similar Solutions for Men Curvature Flow* J. Exper. Math., 3, 1, pp.1-15, 1994.

[9] Chopp, D.L., and Sethian, J.A,. *Flow Under Curvature: Singularity Formation, Minimal Surfaces, and Geodesics*, Jour. Exper. Math., Vol. 2(4), pp. 235–255, 1993.

[10] Evans, L.C., and Spruck, J., *Motion of Level sets by Mean Curvature I*, J. Diff. Geom, Vol. 33, 635, 1991.

[11] Gage, M., *Curve Shortening Makes Convex Curves Circular*, Inventiones Mathematica, Vol. 76, 357, 1984.

[12] Gage, M., and Hamilton, R., *The Equation Shrinking Convex Planes Curves*, J. Diff. Geom, Vol. 23, 69, 1986.

[13] Grayson, M., *The Heat Equation Shrinks Embedded Plane Curves to Round Points*, J. Diff. Geom., Vol. 26, 285, 1987.

[14] Grayson, M., *A Short Note on the Evolution of Surfaces Via Mean Curvatures*, J. Diff. Geom., Vol. 58, 555, 1989.

[15] Huisken, G., *Flow by Mean Curvature of Convex Surfaces into Spheres*, J. Diff. Geom., Vol. 20, 237, 1984.

[16] Kass, M., Witkin, A., and Terzopoulos, D., *Snakes: Active Contour Models*, International Journal of Computer Vision, pp. 321–331, 1988.

[17] Malladi, R., and Sethian, J.A., *Image Processing via Level Set Curvature Flow*, Proc. Natl. Acad. of Sci., USA, Vol. 92(15), pp. 7046–7050, July 1995.

[18] Malladi, R., and Sethian, J.A., *Image Processing: Flows under Min/Max Curvature and Mean Curvature*, Graphical Models and Image Processing, Vol. 58(2), March 1996, in press.

[19] Malladi, R., and Sethian, J.A., *A Unified Approach to Noise Removal, Image Enhancement, and Shape Recovery*, to appear in IEEE Transactions on Image Processing, 1996.

[20] Malladi, R., Sethian, J.A., and Vemuri, B.C., *Evolutionary Fronts for Topology-independent shape Modeling and Recovery*, in Proceedings of Third European Conference on Computer Vision, LNCS Vol. 800, pp. 3–13, Stockholm, Sweden, May 1994.

[21] Malladi, R., Sethian, J.A., and Vemuri, B.C., *Shape Modeling with Front Propagation: A Level Set Approach*, IEEE Trans. on Pattern Analysis and Machine Intelligence, Vol. 17(2), pp. 158–175, Feb. 1995.

[22] Osher, S., and Sethian, J.A., *Fronts Propagating with Curvature Dependent speed: Algorithms Based on Hamilton-Jacobi Formulation*, Journal of Computational Physics, Vol. 79, pp. 12-49, 1988.

[23] Rhee, C., Talbot, L., and Sethian, J.A., *Dynamical Study of a Premixed V flame*, Jour. Fluid Mech., 300, pp. 87-115, 1995.

[24] Sethian, J.A., *An Analysis of Flame Propagation*, Ph.D. Dissertation, Dept. of Mathematics, University of California, Berkeley, 1982.

[25] Sethian, J.A., *Curvature and the Evolution of Fronts*, Comm. in Mathematical Physics, Vol. 101, pp. 487–499, 1985.

[26] Sethian, J.A., *Numerical Methods for Propagating Fronts*, in Variational Methods for Free Surface Interfaces, edited by P. Concus and R. Finn, Springer-Verlag, New York, 1987.

[27] Sethian, J.A., *Numerical Algorithms for Propagating Interfaces: Hamilton-Jacobi Equations and Conservation Laws*, Journal of Differential Geometry, Vol. 31, pp. 131–161, 1990.

[28] Sethian, J.A., *Curvature Flow and Entropy Conditions Applied to Grid Generation*, J. Comp. Phys. Vol. 115, pp.440-454, 1994.

[29] Sethian, J.A., *Level Set Techniques for Tracking Interfaces; Fast Algorithms, Multiple Regions, Grid Generation and Shape/Character Recognition*, Proceedings of Second Trento Conference on Mean Curvature Motion, July, 1994.

[30] Sethian, J.A., *Algorithms for Tracking Interfaces in CFD and Material Science*, Annual Review of Computational Fluid Mechanics, 1995.

[31] Sethian, J.A., *A Fast Marching Level Set Method for Monotonically Advancing Fronts*, Proceedings of the National Academy of Sciences, 93, 4, 1996.

[32] Sethian, J.A., *A Review of the Theory, Algorithms, and Applications of Level Set Methods for Propagating Interfaces*, to appear, in press, Acta Numerica, 1995.

[33] Sethian, J.A., *Level Set Methods: Evolving Interfaces in Geometry, Fluid Mechanics, Computer Vision and Material Science*, in press, Cambridge University Press, 1996.

[34] Sethian, J.A., Malladi, R., Adalsteinsson, D., and Kimmel, R., *Fast Marching Methods for Computing Solutions to Static Hamilton-Jacobi Equations*, submitted for publication, SIAM Journal of Numerical Analysis, Jan. 1996.

[35] Sethian, J.A. and Strain, J.D., *Crystal Growth and Dendritic Solidification* J. Comp. Phys., Vol. 98, pp. 231-253, 1992.

[36] Zhu, J., and Sethian, J.A., *Projection Methods Coupled to Level Set Interface Techniques*, J. Comp. Phys., vol. 102, pp. 128-138, 1992.